

Document Version

Final published version

Licence

CC BY

Citation (APA)

Kabakcı, Y. G., Mehtap, N., Kabatas, M. A. B. M., & Kılıç, H. Ş. (2026). Eco-friendly PAN/collagen photocatalytic nanofibers reinforced with femtosecond laser-synthesized TiO₂@ag nanoparticles for Plasmon-enhanced wastewater treatment. *Colloids and Interface Science Communications*, 73, Article 100903. <https://doi.org/10.1016/j.colcom.2026.100903>

Important note

To cite this publication, please use the final published version (if applicable). Please check the document version above.

Copyright

In case the licence states "Dutch Copyright Act (Article 25fa)", this publication was made available Green Open Access via the TU Delft Institutional Repository pursuant to Dutch Copyright Act (Article 25fa, the Taverne amendment). This provision does not affect copyright ownership. Unless copyright is transferred by contract or statute, it remains with the copyright holder.

Sharing and reuse

Other than for strictly personal use, it is not permitted to download, forward or distribute the text or part of it, without the consent of the author(s) and/or copyright holder(s), unless the work is under an open content license such as Creative Commons.

Takedown policy

Please contact us and provide details if you believe this document breaches copyrights. We will remove access to the work immediately and investigate your claim.



Eco-friendly PAN/collagen photocatalytic nanofibers reinforced with femtosecond laser-synthesized TiO₂@Ag nanoparticles for Plasmon-enhanced wastewater treatment[☆]

Yasemin Gündoğdu Kabakçı^{a,b,c}, Nezihe Mehtap^a, M.A.Basyooni-M. Kabatas^{d,e,f,*}, Hamdi Şükür Kılıç^g

^a Department of Physics, Faculty of Science, Selçuk University, Konya, Turkey

^b Laser Induced Proton Therapy Application and Research Center, Selçuk University, Konya, Turkey

^c High Technology Research and Application Center, Selçuk University, Konya, Turkey

^d Department of Precision and Microsystems Engineering, Delft University of Technology, Mekelweg 2, 2628 CD Delft, Netherlands

^e Institute of Nanotechnology (INT), Karlsruhe Institute of Technology (KIT), Kaiserstraße 12, 76131 Karlsruhe, Germany

^f Department of Nanotechnology and Advanced Materials, Graduate School of Applied and Natural Sciences, Selçuk University, Konya 42030, Turkey

^g Department of Metallurgical and Materials Engineering, Faculty of Engineering, Dokuz Eylül University, Central Campus, Buca, İzmir, Turkey

ARTICLE INFO

Keywords:

Femtosecond laser ablation
TiO₂@Ag nanoparticles
Electrospun PAN/collagen nanofibers
Photocatalysis
Wastewater treatment

ABSTRACT

Silver (Ag) and titanium dioxide (TiO₂) nanostructures were synthesized by femtosecond laser ablation (800 nm, 1 kHz) and incorporated into a polyacrylonitrile (PAN)/collagen blend via electrospinning to obtain functional nanofibrous membranes. The study comprised three stages: nanoparticle synthesis, nanofiber fabrication and characterization, and evaluation of photocatalytic performance. UV-Vis spectroscopy of TiO₂@Ag nanoparticles showed a gradual decrease in absorbance from the ultraviolet to infrared region and an estimated band gap of ~2.5 eV. FTIR analysis (500–3000 cm⁻¹) confirmed successful incorporation of TiO₂@Ag into the PAN/collagen matrix, while SEM revealed uniform nanofibers with an average diameter of ~100 nm. Photocatalytic activity was assessed by the degradation of methylene blue under light irradiation. The PAN/collagen/TiO₂/Ag nanofibers exhibited markedly improved photodegradation efficiency, highlighting the role of nanofiber architecture and plasmon-enhanced photocatalysis in developing advanced materials for wastewater treatment.

1. Introduction

The water and air pollution cause serious environmental and health problems worldwide [1]. The photodegradation process, which is one of the scientific techniques developed for the removal of these organic pollutants from the environment, is an effective, repeatable method in the creation of harmless forms through photocatalytic oxidation [2]. Photocatalytic oxidation is an environmentally friendly catalytic approach that can be performed under normal temperature and pressure, and prevents secondary pollution by completely and rapidly oxidizing organic pollutants to harmless substances such as carbon dioxide and water [3]. Although nanosized photocatalysts have an effect on the decomposition of organic pollutants, powdery forms can reduce photocatalytic activity due to their instability and aggregation, or

complicate the recycling of catalysts, causing secondary contamination and possible cytotoxic effects of remnants of powdery catalysts [4]. For this reason, nanofiber production from various materials containing polymers, metals, and ceramics by the electro-spinning method in photocatalyst preparation is a versatile and widely used approach [1,3].

Electrospinning technology offers a simple and efficient approach for the fabrication of membrane materials [5,6]. Following appropriate treatment, electrospun membranes retain their structural integrity, making them suitable for a wide range of applications, including electronic devices, food preservation, drug delivery, environmental remediation, multifunctional materials, and hydrogen evolution reactions [7–9]. Nanofibrous structures are particularly promising for such applications due to their high surface area and ease of recovery, both of which facilitate the photocatalytic processes required for effective water

[☆] This article is part of a Special issue entitled: 'From Colloids to Clean Energy' published in Colloid and Interface Science Communications.

* Corresponding author at: Department of Precision and Microsystems Engineering, Delft University of Technology, Mekelweg 2, 2628 CD Delft, Netherlands.

E-mail address: m.kabatas@tudelft.nl (M.A.Basyooni-M. Kabatas).

purification. [10].

Cleaning water by selecting non-toxic materials is crucial to prevent secondary pollution. In this regard, the non-toxicity of titanium dioxide (TiO₂) and silver (Ag) nanoparticles (NPs), and their presence of electron-hole vacancies, are particularly valuable for investigating photocatalytic effects. TiO₂ and Ag NPs are generally synthesized using either chemical or physical methods [11,12]. While chemical approaches often involve complex procedures and potentially hazardous reagents, physical methods such as thermolysis, radiolysis, and laser ablation offer simpler, cleaner alternatives [13]. Among these, femtosecond (fs) laser ablation has gained particular attention due to its ability to produce stable, long-lasting NP dispersions in a relatively short time and under ambient conditions [14]. Furthermore, since the laser beam directly interacts with the target material, the resulting NPs exhibit high purity. This method is also applicable, as it can be used with multiple targets across various solvent environments [15,16]. TiO₂, an environmentally friendly semiconductor photocatalyst, is widely used in operations such as water treatment, air purification, and disinfection due to its stable structure, high activity, non-toxicity, and low cost [3,17,18]. Studies have shown that Ag-doped TiO₂ materials can enhance interface load transfer, in addition to their antibacterial properties, and expand their working range into the visible-light region, thereby increasing photocatalytic activity [19]. Ag is among the most widely used metals in health, the semiconductor industry, and scientific research due to its antibacterial properties and, especially, its biocompatibility [20,21]. Electrospun polyacrylonitrile (PAN) nanofibers are long, one-dimensional nanostructures with good chemical stability and excellent flexibility [22]. PAN-based hybrid nanofibers can be easily removed from the solution [22,23]. Collagen, known for its good biocompatibility and cell-adhesion properties, has become important for biomedical applications and tissue engineering due to its structural and fiber-form features in the extracellular matrix. The biodegradability, non-toxicity, and biocompatibility of collagen biomaterials address potential biocompatibility concerns. Moreover, collagen-based nanofibers represent a significant natural biomaterial for wound healing, and their advantages should not be overlooked regardless of the production method employed [24,25].

In this study, the synthesis of TiO₂ NPs and Ag NPs by the fs laser ablation method, which represents a green synthesis approach for nanoparticle production, as it eliminates the need for chemical reducing agents or stabilizers, operates under ambient conditions, and enables the generation of high-purity nanoparticles with minimal environmental impact, was carried out in *N,N*-dimethylformamide (DMF) solvent. The TiO₂ and Ag NPs synthesized in this study were successfully incorporated into a PAN/collagen polymer matrix and fabricated via the electrospinning technique, which is a highly effective and versatile method for producing uniform nanofibrous structures with high surface area, enhanced nanoparticle dispersion, and facile recovery, thereby significantly improving their applicability in photocatalytic systems. The FTIR spectra were recorded to characterize the structural properties of the fabricated nanofibers. In addition, their surface morphologies were examined using scanning electron microscopy (SEM). Moreover, the photocatalytic activities of PAN/collagen/TiO₂/Ag composite nanofibers were thoroughly assessed in the MB degradation process. Fs laser ablation method -characterized by minimal chemical usage, rapid nanoparticle production, and environmental friendliness -was employed to elucidate their potential in environmental remediation applications.

2. Materials and methods

2.1. Experimental materials for TiO₂@Ag Nps doped PAN/collagen nanofibers

In this study, PAN (Sigma-Aldrich) and Type I collagen (Sigma-Aldrich) were selected as the polymer; TiO₂ (Kurt Lesker) and Ag (Kurt Lesker) sputtering targets with 99.9% purity were purchased for fs

laser ablation in dimethylformamide (DMF) solvent. MB dye (Sigma-Aldrich) was used for photocatalytic activation.

2.2. Femtosecond laser ablated NP production

This study comprises four experimental stages. In the first stage, Ag and TiO₂ NPs were produced via fs laser ablation. In the second stage, the produced NPs were incorporated into polymers, and nanofibers were obtained via electrospinning. In this stage, data analysis and catalyst characterization. In the final stage, photocatalysis studies were conducted for MB degradation. Ag and TiO₂ targets (purity >99%) were used, and 6 mL of DMF was added to a glass Petri dish using a syringe.

The femtosecond laser system used in this study consists of an amplifier (Quantronix, Integra-C, NY) and a laser head (Quantronix, Ti-Light, NY) and operates at a fundamental wavelength of 800 nm with a repetition rate of 1 kHz, delivering a maximum average laser power of 3.5 W. An integrated laser micromachining unit, equipped with an F-theta lens and a computer-controlled translation stage, enables nanoparticle production via the laser ablation method, as schematically illustrated in the corresponding in Fig. 1a. When the fs laser beam is directed to the micromachining unit, the F-theta lens focuses the beam at an approximate focal distance of 11 cm. For nanoparticle synthesis, a laser power of 650 mW was employed, corresponding to a laser fluence of 2.25 J/cm² and a laser intensity of 7.97×10^{12} W/cm². Under these ablation conditions, the nanoparticle sizes obtained were previously reported by the authors and demonstrated through imaging techniques to range approximately between 50 and 80 nm, consistent with values presented in the literature [14,20]. After the laser ablation process, approximately 150 µg TiO₂ NPs were produced. Similar processes were repeated for Ag NPs in a DMF solution containing approximately 150 µg. Ag and TiO₂ NPs were mixed using a magnetic stirrer at 240 rpm. Following mixing, the solution was sealed with parafilm to prevent exposure to the external atmosphere.

2.3. Production of PAN/collagen/ TiO₂/ag nanofibers by electrospinning method

Within the scope of this study, the electrospinning method was used to produce nanofibers. In this method, after a suitable polymer solution is prepared, it is converted into nanofibers, as shown in Fig. 1b. A PAN-collagen polymer mixture was used to produce nanofibers. In this technique, by placing the aluminum foil cut to the dimensions of the electrode on the rotating baseplate, the nanofibers formed are collected on the collector electrode surface. The reason for the preference for aluminum foil is that a large electric field (about 50,000 V/m) is applied when high voltage is applied at a certain distance between the needle at the end of the syringe and the collector baseplate, and a conductive material is needed to transmit it. The homogeneous solution prepared was loaded into the syringe for use in the electrospinning device, set to 18 kV, a collector-to-syringe distance of 15 cm, and collected on aluminum foil placed on the cylindrical rotary collector at a flow rate of 0.50 mL/h [26]. A 5 wt% polymer solution was prepared by incorporating PAN and collagen at weight ratios of 80% and 20%, respectively. Subsequently, TiO₂@Ag nanoparticles were added to the mixture to achieve a homogeneous dispersion. The process continued for 1 h. Thus, nanofibers were successfully produced. All experiments were conducted at room temperature. All the obtained nanofibers were placed in a petri dish and made suitable for photocatalysis studies. The experimental procedures for the nanofibers produced in this study have been described in detail in our previous work [26,27].

2.4. Photocatalytic activity measurements of TiO₂@Ag Nps doped PAN/collagen nanofibers

In the presence of the obtained nanofiber photocatalysts, the degradation process of MB paint was examined. The experiments were

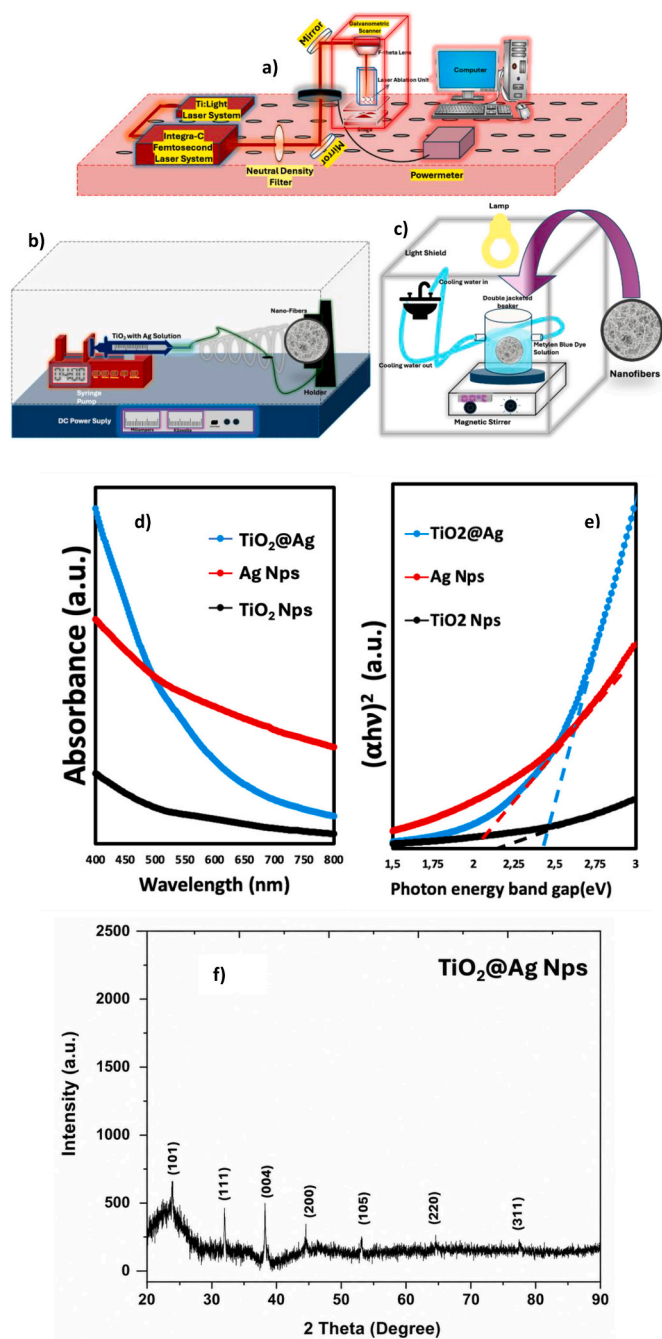


Fig. 1. a) Femtosecond laser-based NP production set-up, b) nanofiber production has been conducted using the electrospinning method, c) photocatalysis experimental set-up for MB degradation, d) Uv-vis absorbance of $\text{TiO}_2\text{@Ag}$ Nps, which were synthesized using fs laser ablation, e) photon energy band gap graph for $\text{TiO}_2\text{@Ag}$ Nps, e) XRD graph shows $\text{TiO}_2\text{@Ag}$ Nps consist of crystalline anatase TiO_2 and metallic Ag phases.

performed under visible light using the MB (10 mg L^{-1}) dye solution. During the photocatalysis process, all samples at pH 10 were analyzed by measuring absorption spectra under visible light. In photocatalysis experiments, the nanofibers' photocatalytic activity was investigated under a 250 W metal halide lamp for the degradation of MB To investigate the photocatalytic performance of $\text{TiO}_2\text{@Ag}$ Nps PAN/collagen nanofibers under Vis light at room temperature, photocatalysts (5 mg) were weighed into a specified amount of MB solution and stirred for 30 min to achieve adsorption-desorption equilibrium. The distance between the light source and the liquid surface was fixed at 15 cm (Fig. 1c).

At predetermined illumination intervals, the concentration of MB was monitored using a UV-Vis absorbance spectrophotometer.

A 100 mL dye solution at 10 ppm was prepared in a beaker, and nanofiber samples ($4 \times 4 \text{ cm}^2$) were uniformly distributed and subsequently immersed in a 50-ppm dye solution. The photocatalytic reaction was then initiated by irradiation with a lamp. Dye concentrations were measured using absorption spectra taken by a UV-Vis spectrophotometer (Shimadzu UV-3101 Spectrometry) with samples that were then removed (at different intervals).

3. Results and discussion

In this study, a UV-Vis Spectrometer was used to determine the absorbance of NPs produced using fs laser ablation, as shown in Fig. 1d. The absorbance of NPs $\text{TiO}_2\text{@Ag}$ decreases from the UV region to the Vis region. Energy band gap values of the catalyst were also calculated to be 2.5 eV using Tauc plotting presented in Fig. 1e [28]. In the XRD graph, 1f, The (101) crystal plane of the anatase TiO_2 phase was identified by the XRD analysis as the source of a distinctive diffraction peak at about 25.3° . The (004), (105), and (204) planes of anatase TiO_2 were associated with additional diffraction peaks at approximately 37.8° , 53.9° , and 62.7° , respectively. Additionally, the (111), (200), (220), and (311) planes of face-centered cubic (fcc) Ag nanoparticles are represented by the diffraction peaks seen at roughly 38.1° , 44.3° , 64.4° , and 77.4° , respectively. These results verify the presence of crystalline anatase TiO_2 and metallic Ag phases in the $\text{TiO}_2\text{@Ag}$ Nps produced using the femtosecond laser ablation technique.

The scanning electron microscope (SEM) (Zeiss Evo LS10) was used to determine the surface morphology of the nanofibers produced. SEM images were obtained for the Ag Nps doped PAN/collagen nanofibers with 80 KX, TiO_2 Nps doped PAN/collagen nanofibers with 80 KX, and PAN/collagen/ $\text{TiO}_2\text{@Ag}$ Nanofibers with 10 KX samples, respectively, as presented in Fig. 2a, b, and c. Examination of the surface morphology reveals a homogeneous nanofiber formation in all samples. The average nanofiber diameter of all produced nanofibers ranges from 50 nm to 130 nm, and detailed SEM images of the fabricated nanofibers are presented. The Fourier Transform Infrared (FTIR) spectra were recorded to investigate the chemical structure, functional groups, and interfacial interactions within the PAN/collagen/Ag-doped TiO_2 composite nanofibers presented in Fig. 2d. The obtained spectrum clearly confirms the successful incorporation of polymeric constituents and inorganic nanoparticles without degradation of their characteristic chemical functionalities. The absorption peaks located at approximately 2920 and 2850 cm^{-1} correspond to the asymmetric and symmetric stretching vibrations of aliphatic $-\text{CH}_2$ and $-\text{CH}_3$ groups, primarily associated with the collagen and PAN polymer backbones [29]. The presence of these peaks confirms that the electrospinning and nanoparticle incorporation processes did not disrupt the aliphatic polymer structure. A sharp and well-defined peak at around 2000 cm^{-1} is assigned to the characteristic $-\text{C} \equiv \text{N}$ stretching vibration of polyacrylonitrile (PAN). The retention of this nitrile peak indicates that the PAN molecular structure remains chemically intact after the incorporation of collagen and $\text{TiO}_2\text{@Ag}$ Nps, thus preserving the mechanical integrity and structural stability of the nanofiber matrix.

In the region between 1650 and 1540 cm^{-1} , two prominent absorption bands are observed and attributed to the Amide I and Amide II bands of collagen, respectively. The Amide I band ($\sim 1650 \text{ cm}^{-1}$) arises mainly from $\text{C}=\text{O}$ stretching vibrations, while the Amide II band ($\sim 1540 \text{ cm}^{-1}$) is associated with $\text{N}-\text{H}$ bending and $\text{C}-\text{N}$ stretching vibrations. Slight peak broadening and minor shifts in these bands suggest intermolecular interactions between collagen, PAN chains, and TiO_2 nanoparticles, indicating effective interfacial compatibility within the composite system [30]. The low-wavenumber region between 600 and 500 cm^{-1} exhibits characteristic absorption bands corresponding to $\text{Ti}-\text{O}$ and $\text{Ti}-\text{O}-\text{Ti}$ lattice vibrations, confirming the presence of TiO_2 nanoparticles within the nanofiber matrix [31]. Although Ag

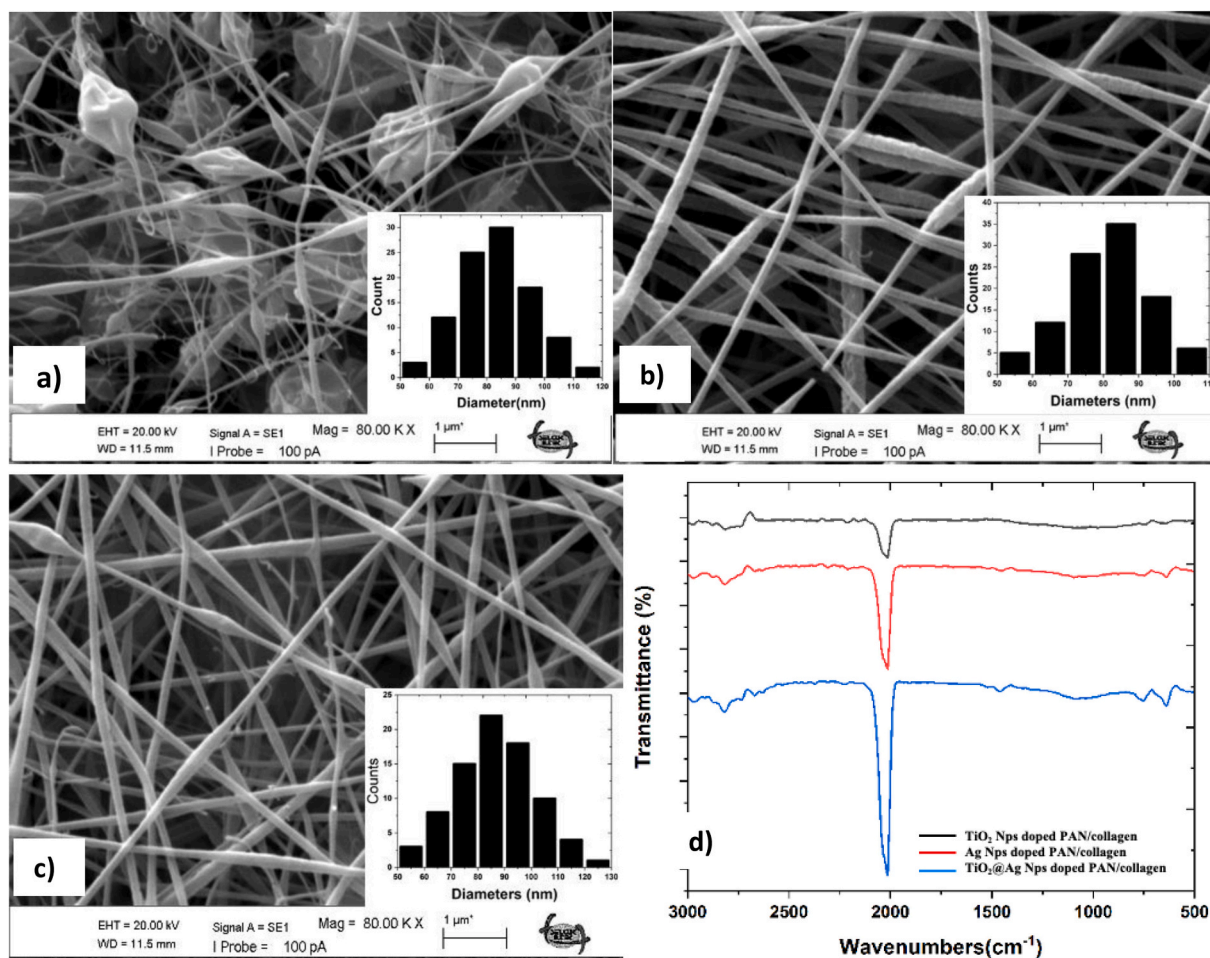


Fig. 2. SEM images were recorded for a) Ag Nps doped PAN/collagen nanofibers with 80 KX, b) TiO₂ Nps doped PAN/collagen nanofibers with 80 KX, c) TiO₂@Ag Nps doped PAN/collagen nanofibers with 80 KX, d) FTIR spectra were taken for TiO₂ Nps doped PAN/collagen, Ag Nps doped PAN/collagen, TiO₂/Ag Nps doped PAN/collagen nanofibers.

nanoparticles do not exhibit distinct FTIR absorption peaks due to their metallic nature, their incorporation influences the local chemical environment of TiO₂, often resulting in subtle changes in band intensity and broadening in this region. This observation indirectly supports the successful formation of TiO₂@Ag within the composite nanofibers. The linear absorbance spectrum shown in Fig. 3a shows MB degradation in the TiO₂@Ag Nps-doped PAN/collagen nanofibers sample at pH 10. It was observed that the absorbance at 240 min was effective for adsorbing the produced nanofibers. This indicates that the nanofibers were successful for MB degradation [32]. The percentage effect of the NPs produced by the laser ablation method on MB degradation is shown in Fig. 3b. The results in Table 1 exhibit that the percent efficiency of TiO₂@Ag Nps doped PAN/collagen nanofibers was 79.55%, while the other PAN/collagen polymers were only 77.97%. The R² correlation coefficients were 0.861 and 0.798 for the TiO₂@Ag Nps doped PAN/collagen and PAN/collagen nanofibers, respectively. This demonstrates the photocatalytic performance of NPs produced by fs laser ablation, known as a clean and environmentally friendly approach, and a successful result was observed in this study.

The following equation was used to evaluate the degradation kinetics of MB for TiO₂@Ag Nps doped PAN/collagen, PAN/collagen, Ag Nps doped PAN, and TiO₂ Nps doped PAN.

$$\ln(C_t/C_0) = -kt$$

Here, k , t , C_0 , and C_t denote the kinetic constant, time, the initial equilibrium concentration of MB, and the concentration of MB at a given time t (e.g., 240 min), respectively. The photocatalytic decay kinetics

have been examined by considering the degradation mechanism observed for all the obtained nanofibers in MB, and these values are presented in Fig. 3c. The change in the kinetic constant over 240 min on a log scale is shown in Fig. 3d.

When irradiated with sufficient light energy, electrons in the valence band (VB) of the photocatalyst are promoted to the conduction band (CB), thereby generating electron-hole pairs that drive subsequent photocatalytic reactions on the surface. These charge carriers migrate to the interface between the photocatalyst and the surrounding environment, initiating redox reactions that generate reactive hydroxyl radicals ($\cdot\text{OH}$). Due to their high reactivity, these radicals effectively degrade pollutants by breaking down the aromatic rings and organic bonds within dye molecules.

The photocatalytic performance is enhanced by increased free-radical generation, which supports more efficient degradation pathways. The proposed mechanism of photocatalytic activity for the synthesized material is illustrated in Fig. 4. The 240-min photocatalytic experiment involving MB degradation confirms the photocatalytic efficiency of TiO₂@Ag NPs embedded in a PAN/collagen polymer matrix.

TiO₂ and Ag nanoparticles were successfully synthesized by laser ablation and subsequently embedded in a PAN/collagen polymer matrix to form a nanocomposite. The photocatalytic activity of this system was evaluated by measuring MB degradation under irradiation. The results demonstrated that the nanocomposite achieved a degradation efficiency of 79.55% after 240 min. This enhanced performance can be attributed to the synergistic effect between TiO₂ and Ag nanoparticles, where Ag acts as an electron sink, improving charge separation and reducing

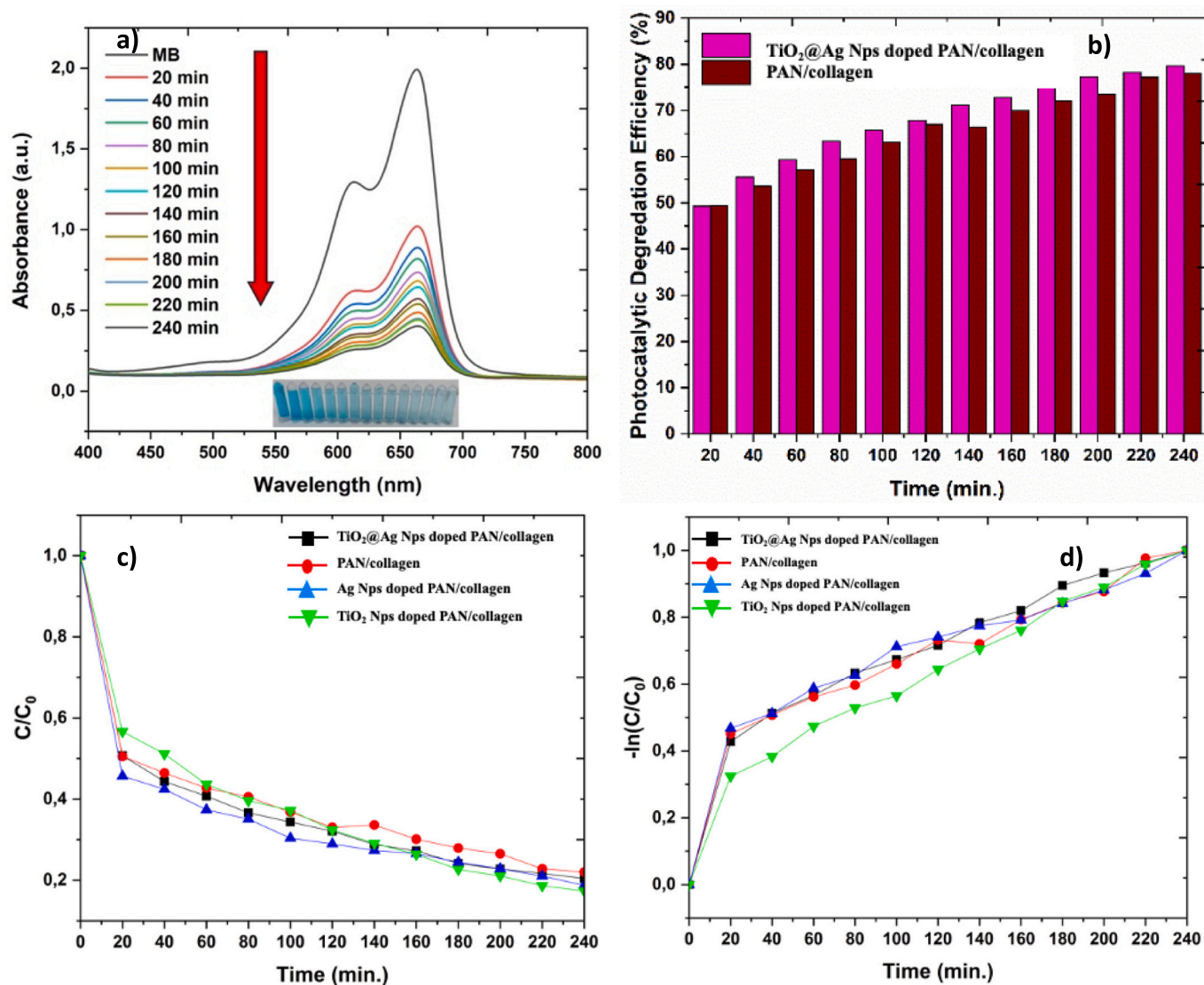


Fig. 3. a) TiO_2/Ag Nps doped PAN/collagen nanofibers absorption performance for MB degradation during 240 min with pH:10, b) Photocatalytic degradation efficiency of both TiO_2/Ag Nps doped PAN/collagen and PAN/collagen nanofibers, c) all samples' efficiency depending on applied time, d) The plot of the log of all samples with time.

Table 1

TiO_2/Ag Nps doped PAN/collagen and PAN/collagen nanofibers for pH:10 kinetic constants, degradation efficiency, and correlation coefficients values.

| Photocatalyst | Kinetic constants, k (min^{-1}) | Photocatalytic degradation efficiency (%) in 240 min) | Correlation coefficient, R^2 |
|---|--|---|--------------------------------|
| TiO_2/Ag Nps doped PAN/collagen | 0.0051 | 79.55 | 0.861 |
| PAN/collagen | 0.0047 | 77.97 | 0.798 |

electron-hole recombination. Compared to pristine TiO_2 -based systems reported in the literature, the obtained degradation efficiency indicates a significant improvement, highlighting the effectiveness of the developed composite structure.

Compared with pristine TiO_2 , PAN-based nanofibrous systems containing TiO_2/Ag NPs exhibit significantly improved photocatalytic performance for MB degradation. This is mainly because of improved charge separation, plasmonic sensitization, and Ag's electron-sink function [19,33,34]. The large surface area and consistent dispersion of nanoparticles, electrospun PAN composites enable the effective production of reactive oxygen species like $\bullet\text{OH}$ and $\text{O}_2^{\bullet-}$, which cause dye oxidation [35]. Depending on experimental factors like light source and catalyst loading, reported TiO_2/Ag Nps doped PAN nanofibers systems

usually produce significant MB degradation within irradiation periods ranging from tens to hundreds of minutes [36,37]. The TiO_2/Ag Nps doped PAN/collagen nanocomposite developed in this work, produced by laser ablation and incorporated into a hybrid polymer matrix, shows 79.55% MB degradation after 240 min. Compared with pristine TiO_2 systems, this performance is competitive and consistent with the literature, demonstrating that the synergistic interaction between TiO_2 and Ag, along with the structural advantages of the PAN/collagen matrix, greatly increases photocatalytic efficiency.

Significant variations in the interfacial charge transfer behavior of the produced nanofibrous membranes were shown by the Nyquist plots (Electrochemical Impedance Spectroscopy- EIS) in Fig. 4b. Higher charge transfer resistance and slower electron transport were shown by

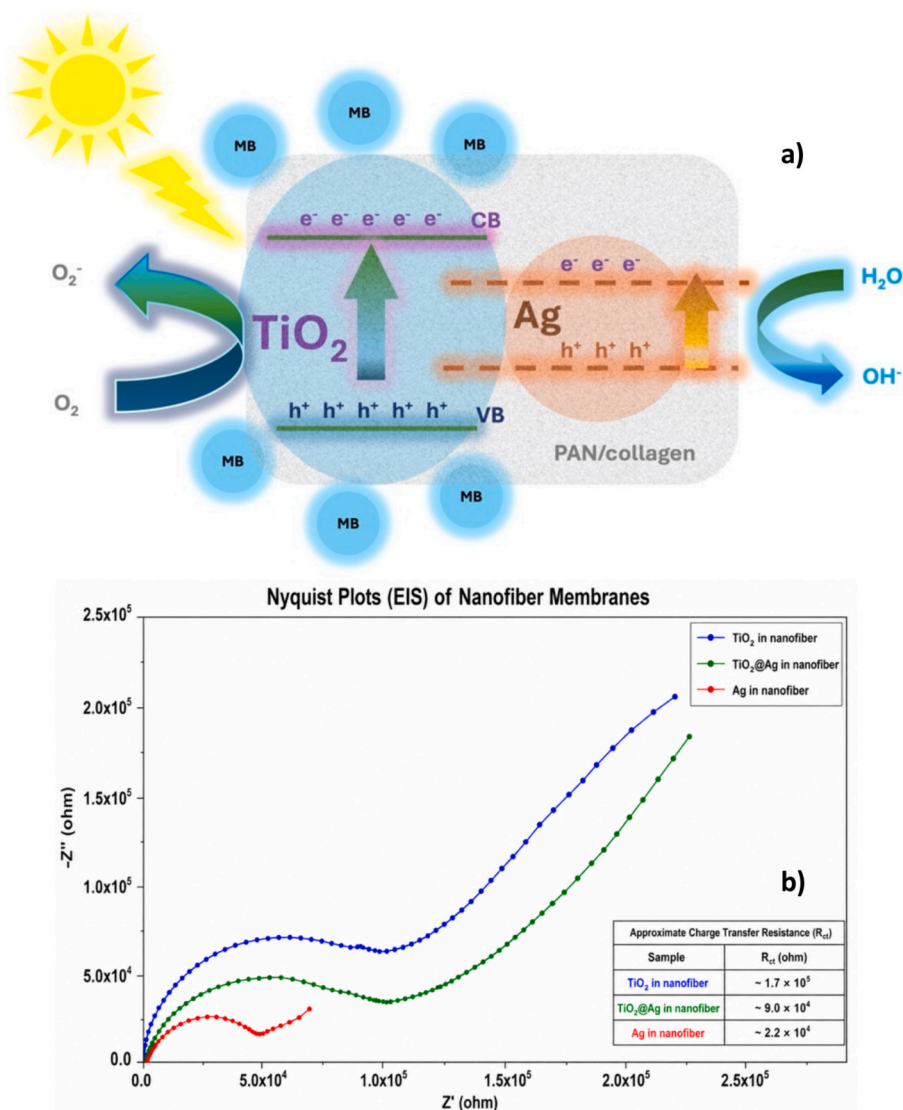


Fig. 4. a) Schematic diagram of the expected MB degradation mechanism of TiO₂/Ag Nps doped PAN nanofibers, b) Nyquist plots have been given for TiO₂/Ag Nps doped PAN nanofibers, Ag Nps doped PAN/collagen nanofibers, TiO₂ Nps doped PAN/collagen nanofibers.

the TiO₂ Nps doped PAN/collagen nanofibers sample's bigger impedance response and prominent diffusion-controlled area [38]. The Ag Nps-doped PAN/collagen nanofiber membrane, on the other hand, displayed a smaller semicircle diameter, indicating improved electrical conductivity and faster interfacial electron transport, as Ag nanoparticles are conductive. Ag nanoparticles successfully promoted charge separation and inhibited electron-hole recombination in the TiO₂ structure in the TiO₂@Ag Nps doped PAN/collagen nanocomposite, exhibiting intermediate behavior [39]. As a result, when compared to TiO₂, the TiO₂@Ag Nps integrated membrane demonstrated better electrochemical performance, which is anticipated to enhance photocatalytic activity [40].

4. Conclusion

This study demonstrates that femtosecond (fs) laser ablation and electrospinning are powerful, environmentally friendly techniques for the design of advanced photocatalytic materials. Fs laser ablation offers a rapid, efficient, and chemical-free route to nanoparticle synthesis, while electrospinning enables precise nanofiber fabrication and the homogeneous embedding of nanoparticles within polymer matrices. Using these approaches, PAN/collagen and TiO₂@Ag Nps doped PAN/

collagen nanofibers were successfully produced. Structural and morphological analyses confirmed the formation of uniform fibers with average diameters of about 100 nm, underscoring the reliability of the electrospinning process for generating well-defined fibrous architectures. FTIR spectra in the 500–3000 cm⁻¹ range revealed the expected functional groups and confirmed the effective incorporation of TiO₂@Ag Nps into doped PAN/collagen nanofibers. Photocatalytic tests showed that TiO₂@Ag Nps doped PAN/collagen nanofibers significantly outperformed pristine PAN/collagen fibers in degrading methylene blue in aqueous solution. This enhancement highlights the key roles of nanofiber morphology, structural stability, and nanoparticle loading in governing photocatalytic activity. Overall, the results point to laser-generated nanoparticle-based nanofibrous systems as promising, sustainable candidates for efficient removal of organic contaminants from wastewater.

CRediT authorship contribution statement

Yasemin Gündoğdu Kabakcı: Writing – original draft, Methodology, Investigation, Conceptualization. **Nezihe Mehtap:** Visualization, Validation, Resources, Investigation. **M.A.Basyooni-M. Kabatas:** Writing – review & editing, Writing – original draft, Visualization,

Resources, Investigation. **Hamdi Şükür Kılıç:** Writing – review & editing, Visualization, Supervision, Project administration, Methodology.

Consent to participate

Not applicable.

Consent for publication

Not applicable.

Funding

Selcuk University Scientific Research Project (BAP) Coordination for the support with project no. 23201008.

Declaration of competing interest

The authors declare that they have no known competing financial interests or personal relationships that could have appeared to influence the work reported in this paper.

Data availability

Data will be made available on request.

References

- H.M. Hassan, et al., Electrospun TiO₂-GO/PAN-CA nanofiber mats: a novel material for remediation of organic contaminants and nitrophenol reduction, *Environ. Res.* 234 (2023) 116587.
- J. Cai, H. Li, Electrospun polymer nanofibers coated with TiO₂ hollow spheres catalyze for high synergistic photo-conversion of Cr (VI) and as (III) using visible light, *Chem. Eng. J.* 398 (2020) 125644.
- X. Li, S. Raza, C. Liu, Directly electrospinning synthesized Z-scheme heterojunction TiO₂@ ag@ Cu₂O nanofibers with enhanced photocatalytic degradation activity under solar light irradiation, *J. Environ. Chem. Eng.* 9 (5) (2021) 106133.
- Y. Shi, et al., Fabrication of PAN@ TiO₂/ag nanofibrous membrane with high visible light response and satisfactory recyclability for dye photocatalytic degradation, *Appl. Surf. Sci.* 426 (2017) 622–629.
- P. Chen, et al., Electrospinning polyacrylonitrile (PAN) based nanofibrous membranes synergic with plant antibacterial agent and silver nanoparticles (AgNPs) for potential wound dressing, *Mater. Today Commun.* 31 (2022) 103336.
- B. Yu, et al., Electrospun hydrophilic PAN/CO/TA composite nanofibrous membrane for adsorbing cu (II) in water, *Polymer* 316 (2025) 127829.
- A.E. Alprol, et al., Melamine-maleic acid polyamide adduct/polyacrylonitrile nanofibers as a novel adsorbent for removal of methylene blue dye from aqueous solutions, *Water Air Soil Pollut.* 235 (7) (2024) 425.
- P. Cui, et al., Advanced review on type II collagen and peptide: preparation, functional activities and food industry application, *Crit. Rev. Food Sci. Nutr.* 64 (30) (2024) 11302–11319.
- Y. Wakuda, et al., Native collagen hydrogel nanofibres with anisotropic structure using core-shell electrospinning, *Sci. Rep.* 8 (1) (2018) 6248.
- S. Ma, A. Li, L. Pan, Application progress of multi-functional polymer composite nanofibers based on electrospinning: a brief review, *Polymers* 16 (17) (2024) 2459.
- K. Natarajan, Antibiofilm activity of epoxy/ag-TiO₂ polymer nanocomposite coatings against *Staphylococcus aureus* and *Escherichia coli*, *Coatings* 5 (2) (2015) 95–114.
- H.F. Moafi, A.F. Shojaie, M.A. Zanjanchi, Photoactive behavior of polyacrylonitrile fibers based on silver and zirconium co-doped titania nanocomposites: synthesis, characterization, and comparative study of solid-phase photocatalytic self-cleaning, *J. Appl. Polym. Sci.* 127 (5) (2013) 3778–3789.
- M.E. Shaheen, A.Y. Abdelwahab, Laser ablation in liquids: A versatile technique for nanoparticle generation, *Opt. Laser Technol.* 186 (2025) 112705.
- Y. Gündoğdu, et al., Femtosecond laser ablation synthesis of nanoparticles and nano-hybrides in ethanol medium, *Mater. Today Proc.* 18 (2019) 1803–1810.
- A. Hamad, L. Li, Z. Liu, A comparison of the characteristics of nanosecond, picosecond and femtosecond lasers generated ag, TiO₂ and au nanoparticles in deionised water, *Appl. Phys. A* 120 (4) (2015) 1247–1260.
- R. Zhou, et al., Continuous synthesis of ag/TiO₂ nanoparticles with enhanced photocatalytic activity by pulsed laser ablation, *J. Nanomater.* 2017 (1) (2017) 4604159.
- D. Yu, et al., AgI-modified TiO₂ supported by PAN nanofibers: a heterostructured composite with enhanced visible-light catalytic activity in degrading MO, *Dyes Pigments* 133 (2016) 51–59.
- S. Karagoz, et al., Synthesis of ag and TiO₂ modified polycaprolactone electrospun nanofibers (PCL/TiO₂-ag NFs) as a multifunctional material for SERS, photocatalysis and antibacterial applications, *Ecotoxicol. Environ. Saf.* 188 (2020) 109856.
- L. Wang, et al., Simultaneously enhanced photocatalytic and antibacterial activities of TiO₂/ag composite nanofibers for wastewater purification, *J. Environ. Chem. Eng.* 8 (1) (2020) 102104.
- Y. Gündoğdu, et al., Femtosecond laser-induced production of ZnO@ ag nanocomposites for an improvement in photocatalytic efficiency in the degradation of organic pollutants, *Opt. Laser Technol.* 170 (2024) 110291.
- H. Shi, et al., Boosted photocatalytic performance for antibiotics removal with ag/PW12/TiO₂ composite: degradation pathways and toxicity assessment, *Molecules* 28 (19) (2023) 6831.
- D. Ding, et al., Piezo-photocatalytic flexible PAN/TiO₂ composite nanofibers for environmental remediation, *Sci. Total Environ.* 824 (2022) 153790.
- L. Wang, et al., *Microcystis aeruginosa* synergistically facilitate the photocatalytic degradation of tetracycline hydrochloride and Cr (VI) on PAN/TiO₂/ag nanofiber mats, *Catalysts* 8 (12) (2018) 628.
- A. Spoiala, et al., Collagen/TiO₂-ag composite nanomaterials for antimicrobial applications, *UPB Sci. Bull. Ser. B* 77 (2015) 275–290.
- S. Lo, E. Mahmoudi, M.B. Fauzi, Applications of drug delivery systems, organic, and inorganic nanomaterials in wound healing, *Discover Nano* 18 (1) (2023) 104.
- Ü.Y. Erbasti, et al., Investigation of PAN: hemp stems nanofibers produced by electrospinning method, *Int. J. Pure Appl. Sci.* 8 (2) (2022) 331–341.
- F.B. Sariipek, Y. Gündoğdu, H.Ş. Kiliç, Fabrication of eco-friendly superhydrophobic and superoleophilic PHB-SiO₂ bionanofiber membrane for gravity-driven oil/water separation, *J. Appl. Polym. Sci.* 140 (9) (2023) e53542.
- I. Tunc, et al., Bandgap determination and charge separation in ag@ TiO₂ core shell nanoparticle films, *Surf. Interface Anal.* 42 (6–7) (2010) 835–841.
- A. Mohamed, et al., Photodegradation of ibuprofen, cetirizine, and naproxen by PAN-MWCNT/TiO₂-NH₂ nanofiber membrane under UV light irradiation, *Environ. Sci. Eur.* 30 (1) (2018) 47.
- A. Mpelane, et al., Application of novel C-TiO₂-CFA/PAN photocatalytic membranes in the removal of textile dyes in wastewater, *Catalysts* 10 (8) (2020) 909.
- C.A. Bode-Aluko, et al., Photocatalytic and antifouling properties of electrospun TiO₂ polyacrylonitrile composite nanofibers under visible light, *Mater. Sci. Eng. B* 264 (2021) 114913.
- B. Xu, et al., Electrospinning preparation of PAN/TiO₂/PANI hybrid fiber membrane with highly selective adsorption and photocatalytic regeneration properties, *Chem. Eng. J.* 399 (2020) 125749.
- M.A. Kanjwal, et al., Functionalization of electrospun titanium oxide nanofibers with silver nanoparticles: strongly effective photocatalyst, *Int. J. Appl. Ceram. Technol.* 7 (2010) E54–E63.
- C.I. Covaliu-Mierla, et al., TiO₂-based nanofibrous membranes for environmental protection, *Membranes* 12 (2) (2022) 236.
- V. Melinte, L. Stroea, A.L. Chibac-Scutaru, Polymer nanocomposites for photocatalytic applications, *Catalysts* 9 (12) (2019) 986.
- D. Dalman, et al., Photocatalytic degradation of allura red (AR) with TiO₂ immobilized on solution blow spinning (SBS)-spun TIPP/PVP membranes, in: *Materials Science Forum*, Trans Tech Publ, 2022.
- C. Mendes-Felipe, et al., Hybrid organic-inorganic membranes for photocatalytic water remediation, *Catalysts* 12 (2) (2022) 180.
- M. Blanco, et al., TiO₂-doped electrospun nanofibrous membrane for photocatalytic water treatment, *Polymers* 11 (5) (2019) 747.
- A. Moradi, M. Abrari, M. Ahmadi, Efficiency enhancement in dye-sensitized solar cells through the decoration of electro-spun TiO₂ nanofibers with ag nanoparticles, *J. Mater. Sci. Mater. Electron.* 31 (19) (2020) 16759–16768.
- H. Shi, et al., Polyoxometalate/TiO₂/ag composite nanofibers with enhanced photocatalytic performance under visible light, *Appl. Catal. Environ.* 221 (2018) 280–289.